

Accepted Manuscript

Discovery of [1,2,4]triazolo[3,4-b][1,3,4]thiadiazole derivatives as novel, potent and selective c-Met kinase inhibitors: Synthesis, SAR study, and biological activity

Li Zhang, Jingyun Zhao, Beichen Zhang, Tao Lu, Yadong Chen



PII: S0223-5234(18)30292-7

DOI: [10.1016/j.ejmech.2018.03.049](https://doi.org/10.1016/j.ejmech.2018.03.049)

Reference: EJMECH 10314

To appear in: *European Journal of Medicinal Chemistry*

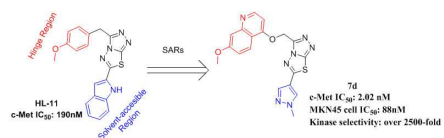
Received Date: 23 January 2018

Revised Date: 17 March 2018

Accepted Date: 17 March 2018

Please cite this article as: L. Zhang, J. Zhao, B. Zhang, T. Lu, Y. Chen, Discovery of [1,2,4]triazolo[3,4-b][1,3,4]thiadiazole derivatives as novel, potent and selective c-Met kinase inhibitors: Synthesis, SAR study, and biological activity, *European Journal of Medicinal Chemistry* (2018), doi: 10.1016/j.ejmech.2018.03.049.

This is a PDF file of an unedited manuscript that has been accepted for publication. As a service to our customers we are providing this early version of the manuscript. The manuscript will undergo copyediting, typesetting, and review of the resulting proof before it is published in its final form. Please note that during the production process errors may be discovered which could affect the content, and all legal disclaimers that apply to the journal pertain.



ACCEPTED MANUSCRIPT

Discovery of [1,2,4]triazolo[3,4-b][1,3,4]thiadiazole derivatives as novel, potent and selective c-Met kinase inhibitors: Synthesis, SAR study, and biological activity

Li Zhang^a, Jingyun Zhao^a, Beichen Zhang^a, Tao Lu^{b,c,*} and Yadong Chen^{b,*}

^a *Department of Organic Chemistry, School of Science, China Pharmaceutical University, 639 Longmian Avenue, Nanjing 211198, China*

^b *Laboratory of Molecular Design and Drug Discovery, School of Science, China Pharmaceutical University, 639 Longmian Avenue, Nanjing 211198, China*

^c *State Key Laboratory of Natural Medicines, China Pharmaceutical University, 24 Tongjiaxiang, Nanjing 210009, China*

Abstract: A series of [1,2,4]triazolo[3,4-b][1,3,4]thiadiazole derivatives were designed, synthesized and evaluated for their biological activity. Most of these compounds showed potent activities against c-Met kinase and cell growth inhibition. The most promising compound, **7d**, has the IC₅₀ values of 2.02 and 88 nM to inhibit c-Met kinase activity and cell growth in the MKN45 cell line, respectively. In addition, **7d** is highly selective to c-Met and exhibits over 2500-fold selective inhibition to 16 tyrosine kinases evaluated.

Keywords: [1,2,4]triazolo[3,4-b][1,3,4]thiadiazole, synthesis, c-Met, inhibitors, SAR

1. Introduction

Mesenchymal-epithelial transition factor (c-Met), the receptor of hepatocyte growth factor (HGF), is a receptor tyrosine kinase (RTK) which plays an important role in cell growth during embryo development and postnatal organ regeneration [1-5]. Overexpression or aberrant activation of c-Met has been reported to be associated with the formation and development of many types of cancers in lung, breast and gastric cancers [6-8]. Consequently, c-Met kinase has been considered as an attractive

target for molecular targeted therapy in cancers. A number of small molecule inhibitors binding to the ATP binding pocket of c-Met protein have been developed to inhibit the activity of c-Met kinase (Fig. 1) [9-14]. Some of them have advanced to the clinical trials currently or have been approved by U.S. Food and Drug Administration [15]. Because of the high homology of RTKs, it remains a challenge to develop a highly selective c-Met inhibitor which is expected to produce less side effects than other RTKs in cancer treatment [16-18].

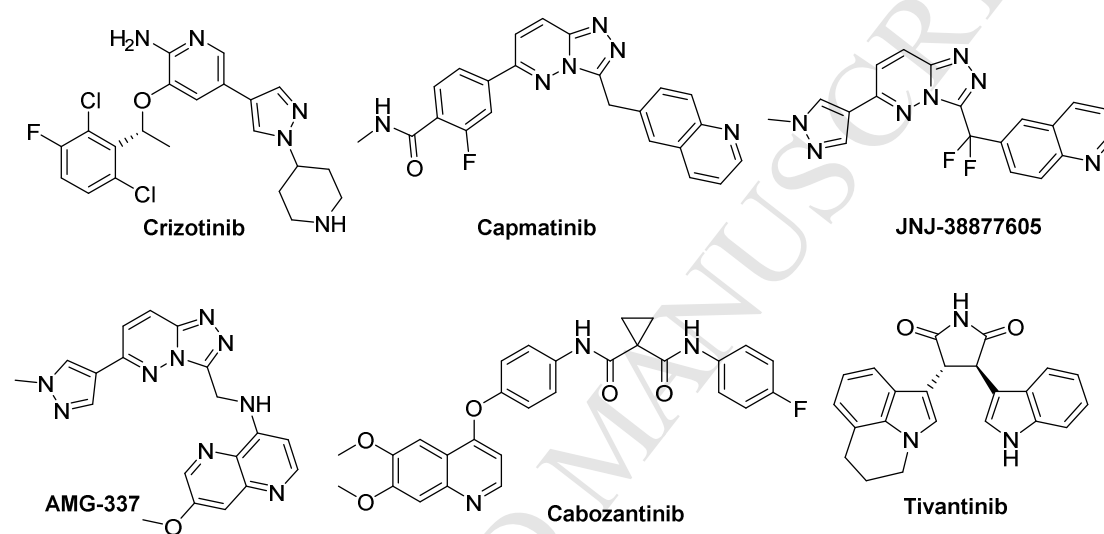


Fig. 1. Structures of reported c-Met kinase inhibitors

In our previous high throughput screening campaign study [19-20], we have discovered a novel c-Met inhibitor, **HL-11**, containing a [1,2,4]triazolo[3,4-b][1,3,4]thiadiazole scaffold that inhibited c-Met kinase at an IC_{50} value of 0.19 μ M. In the crystal structure of compound **HL-11** with c-Met kinase domain (Fig. 2), the [1,2,4]triazolo[3,4-b][1,3,4]thiadiazole group of **HL-11** interacts with Tyr1230 via a π - π staking and forms a hydrogen bond with Asp1222. An important hydrogen bond formed between the oxygen atom of methoxybenzene group in **HL-11** and Met1160 in the hinge region of c-Met protein, was considered to be critical for the inhibition activity of **HL-11** to c-Met. Another hydrogen bond between the N-H on the indole ring of **HL-11** residue Arg1208 is also identified in the crystal structure (Fig. 2).

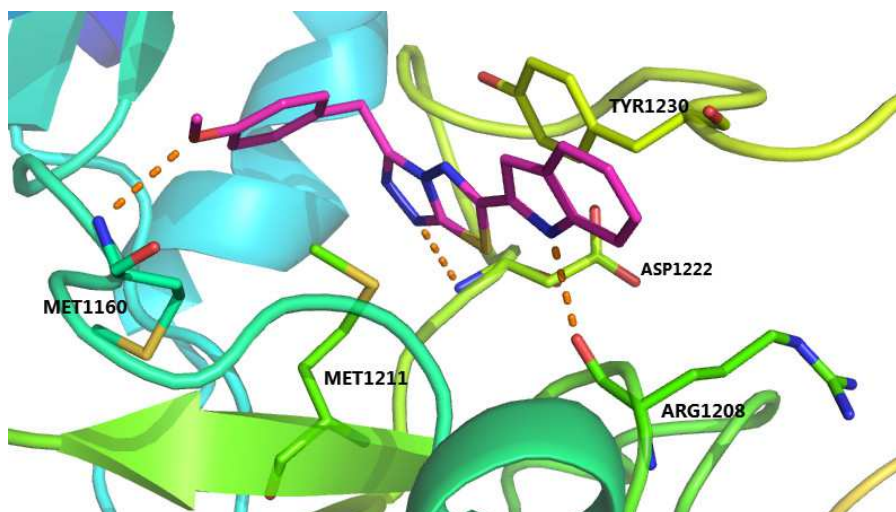


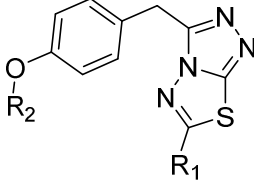
Fig. 2. The crystal structure of **HL-11** in c-Met kinase domain (PDB ID: 5YA5)

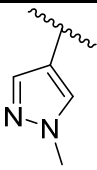
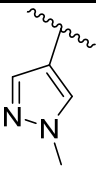
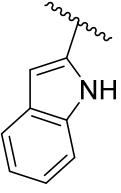
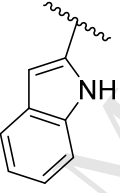
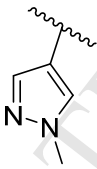
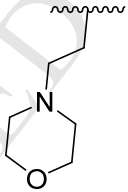
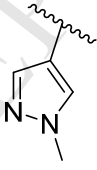
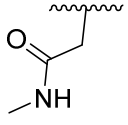
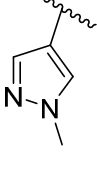
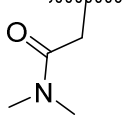
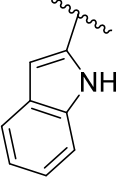
Herein, we designed and synthesized a series of [1,2,4]triazolo[3,4-b][1,3,4]thiadiazole derivatives based on the analysis of the crystal structure between **HL-11** and **c-Met**. These new compounds were evaluated for their inhibition activities to c-Met kinase and cell growth in the PC-3, MKN45 and EBC-1 cancer cell lines. In addition, selectivity profile and inhibition of phosphorylation of c-Met kinase in MKN45 cell line were determined in this work.

2. Chemistry

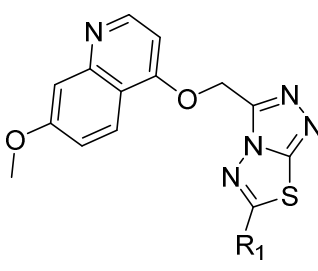
The synthetic routes of **2a**, **2b** and **4a-4c** were shown in Scheme 1. [1,2,4]triazolo[3,4-b][1,3,4]thiadiazole derivatives **2a** and **2b** were readily prepared from a two-step cyclisation of 2-(4-hydroxyphenyl)acetic acid with thiocarbohydrazide and carboxylic acid. Hydrolysis of **2b** with NaOH afforded phenol **3**. Subsequent, treatment of **3** with appropriate chlorides afforded **4a-4c** in the presence of Cs_2CO_3 .

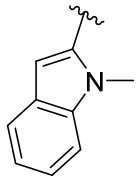
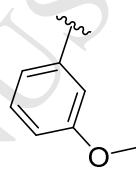
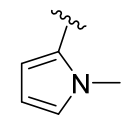
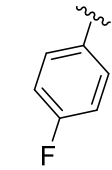
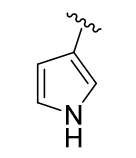
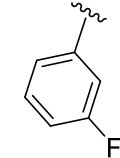
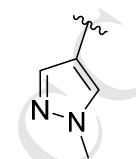
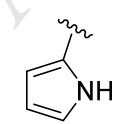
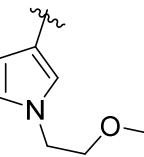
As illustrated in Scheme 2, nucleophilic substitution of 4-Chloro-7-methoxyquinoline and 2-hydroxyacetic acid afforded intermediate **5**. **7a-7m** were prepared from acid **5** using the similar method as those for the preparation of **2a**. Finally, treating **7c** with appropriate bromides in the present of KOH obtained compounds **8a-8c**.

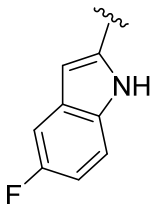
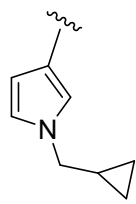
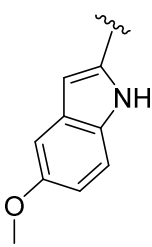
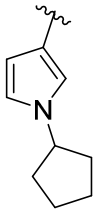
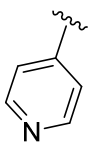
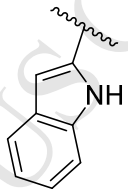
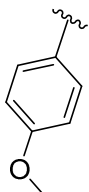
Table 1. Chemical structures of compounds **2a-2b**, **4a-4c** and their c-Met kinase inhibition activities


Compd.	R ₁	R ₂	c-Met kinase IC ₅₀ (μM)
2a			>10
2b			>10
4a			>10
4b			>10
4c			>10
HL-11 ^a		Me	0.19

^a Used as a positive control.

Table 2. Chemical structures of compounds **7a-7m**, **8a-8c** and their c-Met kinase inhibition activities


Compd.	R ₁	c-Met kinase IC ₅₀ (μM)	Compd.	R ₁	c-Met kinase IC ₅₀ (μM)
7a		0.0156	7j		0.0286
7b		0.110	7k		0.0817
7c		0.0167	7l		0.0145
7d		0.00202	7m		0.440
7e		0.0173	8a		0.0314

7f		0.150	8b		0.0273
7g		0.0649	8c		0.201
7h		0.0263	HL-11f		0.0793
7i		0.0145	crizotinib ^a		0.00829

^a Used as a positive control.

The synthesized compounds were evaluated for their c-Met kinase inhibition activity using hot-SpotSM kinase assay method using crizotinib, **HL-11** and **HL-11f** as positive controls. To study the SAR, we investigated several alternative choices of the hinge-binder groups (see the R₂ substituents in Table 1) and a series of hydrophilic groups and aromatic heterocycles installed in the position of methoxy group in **HL-11** to occupy the solvent accessible region. Among compounds in Table 1, **2a**, **2b** and **4a-4c** showed very weak c-Met kinase inhibition activity, indicating that such modification in **HL-11** was not favorable. 7-Methoxyquinolin-4-oxy, a commonly used hinge region group of c-Met inhibitor, was introduced instead of the methoxyphenyl in **HL-11** and several substituted phenyl rings or aromatic heterocyclic rings were assessed to replace the indole ring of **HL-11** (Table 2). The c-Met kinase inhibition activities of **7a** and **11f** showed that the hydrogen bond

between N-H in **HL-11** and Arg1208 was not critical. Compound **7f** with a hydrophobic substituent at the 5-position of indole showed less inhibition activity than **7g** with a hydrophilic or no substituent (**HL-11f**). Compounds **7b-7e**, **7h-7j** and **7l** demonstrated good c-Met kinase inhibition activity, suggesting that the electron density of the aromatic groups in the hydrophilic region have little influence on their kinase inhibition activities. The inhibition to c-Met kinase did not improved when either methoxyethyl (**8a**), cyclopropylmethyl (**8b**) or cyclopentyl (**8c**) were introduced in the pyrrolyl fragment of **7c**. Compound **7d** with N-methyl pyrazole group displayed the highest inhibitory potency giving an IC₅₀ value of 2.02 nM. **7d** was docked to c-Met kinase and the overlaid results revealed that **7d** had a similar binding mode as the lead compound **HL-11** (Fig. 3). Specifically, the [1,2,4]triazolo[3,4-b][1,3,4]thiadiazole groups of **7d** and **HL-11** overlapped almost completely. The quinoline N and the methoxy group of **7d** also formed two hydrogen bonds with residues Met1160 and Tyr1159 respectively.

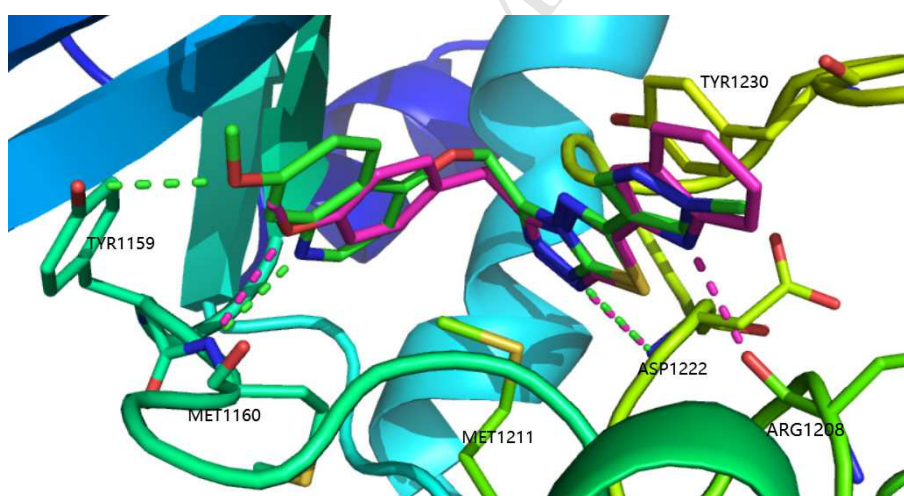


Fig. 3. Binding mode of compound **7d** (green) overlaid with **HL-11** (light magenta) at the c-Met kinase domain. The formed hydrogen bonds were marked with green and light magenta respectively.

3.2 *In vitro* cell growth inhibition assays

Table 3. Cytotoxic activities of compounds **7a-7m** and **8a-8c** against SNU-5, MKN45, EBC-1 cell lines *in vitro*^a

Compd.	Antiproliferative activity at 5 μ M			Antiproliferative activity at 1 μ M		IC ₅₀ (nM)
	SNU-5	MKN45	EBC-1	MKN45	EBC-1	EBC-1
7a	67.7%	74.1%	87.0%	60.8%	91.6%	312.6
7b	14.5%	28.1%	86.3%	ND	7.4%	ND
7c	71.5%	70.5%	85.9%	71.1%	90.6%	353.2
7d	68.7%	71.9%	84.4%	73.6%	90.9%	88
7e	72.4%	76.8%	83.7%	79.3%	80.5%	149
7f	54.4%	47.7%	42.3%	ND	ND	ND
7g	60.0%	61.2%	84.0%	75.3%	82.2%	85.6
7h	65.7%	73.0%	83.7%	73.8%	91.6%	289.2
7i	74.5%	72.0%	85.2%	76.4%	89.1%	161
7j	65.7%	66.6%	85.4%	37.8%	91.5%	472.1
7k	65.8%	71.0%	83.1%	68.5%	89.4%	186.7
7l	66.3%	71.3%	81.4%	13.2%	86.7%	504.3
7m	44.7%	29.8%	84.5%	ND	89.3%	403.3
8a	46.1%	73.0%	78.6%	71.1%	89.0%	327.4
8b	52.2%	66.6%	75.9%	41.1%	87.2%	350.8
8c	42%	47.6%	72.1%	ND	41.3%	ND
HL-11f ^b	70.2%	76.3%	87.3%	78.1%	86.5%	106.6
Crizotinib ^b	80.0%	77.7%	94.4%	82.6%	93.1%	39

^a ND: not determined. ^b Used as a positive control.

The inhibitory effects of compounds **7a-7m** and **8a-8c** were evaluated in several c-Met overexpressed human cancer cell lines, including SNU-5 (human gastric cancer), MKN45 (human gastric cancer) and EBC-1 (human lung cancer) cells [21-23]. The results are summarized in Table 3. Most of the compounds showed potent antiproliferative activity against these cell lines, especially EBC-1 cells. Compounds with indole substituent (**7a**, **7g** and **HL-11f**) showed better cellular potency than compounds with single ring in hydrophilic region (**7b**, **7c**, **7e**, **7h-7m** and **8a-8c**) except **7d**.

3.3 Enzymatic selectivity assays

Table 4. Kinase selectivity profile of compound **8c**

Kinase	Inhibition at 5 μ M	Kinase	Inhibition at 5 μ M
FLT3	69.68% (1.37 μ M)	c-Kit	10.93%
ABL1	14.91%	PDGFR α	-3.29%
AXL	11.11%	EGFR	-10.68%
RON/MST1R	-15.45%	FGFR1	-14.57%
RET	-0.73%	TIE2/TEK	-7.71%
ALK	-1.59%	TRKA	-11.80%
FLT1/VEGFR1	0.28%	TRKB	0.04%
KDR/VEGFR2	-3.93%	LCK	-0.81%

To further examine the selectivity profile of **7d**, **7d** was evaluated against a panel of 16 tyrosine kinases, including FLT3, ABL1, AXL, RON, RET, ALK, FLT1, KDR, c-Kit, PDGFR α , EGFR, FGFR1, TIE2, TRKA, TRKB and LCK. As shown in Table 4, compared to its inhibition activity against c-Met kinase (IC₅₀: 2.02 nM), **7d** demonstrated more than 2500-fold less potency against these selected kinases except FLT3 (IC₅₀: 1.37 μ M, over 650-fold of its c-Met IC₅₀), indicating that **7d** is a highly

selective c-Met inhibitor.

3.4 Western blot analysis

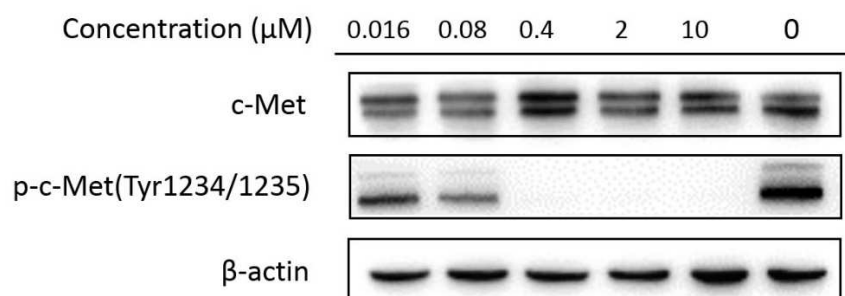


Fig. 4. Compound **7d** inhibited c-Met phosphorylation in MKN45 cells.

We further investigated if c-Met kinase inhibition of **7d** could be recapitulated in vitro in western blotting assay using the MKN45 cell line. MKN45 cells were treated with different doses of **7d** for 1h and the cell lysates were prepared for western blotting analysis [21]. As shown in Fig. 4, compound **7d** inhibited HGF-induced c-Met phosphorylation in a dose-dependent manner in MKN45 cells and c-Met phosphorylation was completely inhibited at a concentration of 0.4 μM.

4. Conclusion

In summary, a series of [1,2,4]triazolo[3,4-b][1,3,4]thiadiazole derivatives were synthesized and evaluated as novel c-Met inhibitors. SAR studies was carried out and compound **7d** was identified as the most potent and selective c-Met inhibitor with an IC_{50} value of 2.02 nM against c-Met kinase activity and gave over 2500-fold selectivity against other 16 tyrosine kinases evaluated. Moreover, **7d** exhibited high antiproliferative activities against several cancer cell lines (SNU-5, MKN45 and EBC-1) and displayed high inhibitory effect on c-Met phosphorylation in the MKN45 cancer cell line. Further optimization and in vivo efficacy experiment of **7d** are currently ongoing in our lab and the results will be reported in due course.

5. Materials and methods

5.1. Instrumentation and chemicals

All reactions were performed under N₂ unless otherwise indicated. Reagents and solvents were purchased as reagent grade and were used without further purification. Flash column chromatography was performed over silica gel (200 - 300 m) using a mixture of ethyl acetate (EA), petroleum ether (PE), dichloromethane (DCM) and MeOH. ¹H NMR and ¹³C NMR spectra were obtained at room temperature using a Bruker Avance 300 spectrometer. The abbreviations s, d, t, q and m signify singlet, doublet, triplet, quartet and multiplet, respectively. Because of the poor solubility, ¹³C NMR analysis of compounds **4a**, **7b**, **7e-7h**, **7l-7m**, **8a-8c** were not applicable. High resolution mass spectrometry (HRMS) was obtained on a Q-TOF micro spectrometer. Melting points were determined with a Micro melting point apparatus. TLC plates were visualized by exposure to ultraviolet light.

5.2. Experimental

5.2.1. General procedure for preparation of **2a-2b**, **4a-4c**, **7a-7m**

The synthesis methods of **2a-2b**, **4a-4c** and **7a-7m** would not be shown here because their preparation has been presented in detail in our previous study [20].

5.2.1.1.

4-((6-(1-methyl-1H-pyrazol-4-yl)-[1,2,4]triazolo[3,4-b][1,3,4]thiadiazol-3-yl)methyl)phenyl 1-methyl-1H-pyrazole-4-carboxylate (2a)

White solid; Yield: 27%; m.p.: 167-168 °C; ¹H NMR (300 MHz, DMSO-*d*₆) δ 8.61 (s, 1H), 8.53 (s, 1H), 8.10 (s, 1H), 8.01 (s, 1H), 7.42 (d, *J* = 8.2 Hz, 2H), 7.18 (d, *J* = 8.0 Hz, 2H), 4.45 (s, 2H), 3.93 (s, 3H), 3.92 (s, 3H); ¹³C NMR (75 MHz, DMSO-*d*₆) δ 161.23, 159.65, 152.83, 149.60, 146.62, 141.33, 138.17, 135.59, 133.63, 132.23, 130.30(2C), 122.59(2C), 113.15, 112.42, 39.49 (2C), 30.21; HRMS (ESI) *m/z* calcd for C₁₉H₁₇N₈O₂S⁺ [M+H]⁺: 421.11897; found: 421.11983.

5.2.1.2.

4-((6-(1H-indol-2-yl)-[1,2,4]triazolo[3,4-b][1,3,4]thiadiazol-3-yl)methyl)phenyl 1H-indole-2-carboxylate (2b)

White solid; Yield: 27%; m.p.: 280-281 °C; ¹H NMR (300 MHz, DMSO-*d*₆) δ 9.35 (s, 1H), 8.60 (s, 1H), 8.09 (s, 1H), 7.14 (d, *J* = 7.9 Hz, 2H), 6.75 – 6.66 (m, 2H), 4.26 (s, 2H), 3.93 (s, 3H); ¹³C NMR (75 MHz, DMSO-*d*₆) δ 160.33, 159.44, 152.95, 149.68,

146.79, 138.62, 138.31, 133.95, 130.41(2C), 127.69, 127.18, 126.82, 126.57, 125.70, 125.55, 122.77, 122.64(2C), 122.06, 121.11, 120.91, 113.16, 112.88, 109.97, 107.94, 30.26; HRMS (ESI) m/z calcd for $C_{27}H_{18}N_6O_2SNa^+$ $[M+Na]^+$: 513.11148; found: 513.11159.

5.2.1.3.

4-(2-(4-((6-(1-methyl-1H-pyrazol-4-yl)-[1,2,4]triazolo[3,4-b][1,3,4]thiadiazol-3-yl)methyl)phenoxy)ethyl)morpholine (4a)

White solid; Yield: 43%; m.p.: 155-157°C; 1H NMR (300 MHz, DMSO- d_6) δ : 8.59 (s, 1H), 8.08 (d, $J = 0.8$ Hz, 1H), 7.31 – 7.20 (m, 2H), 6.95 – 6.84 (m, 2H), 4.32 (s, 2H), 4.05 (t, $J = 5.7$ Hz, 2H), 3.93 (s, 3H), 3.61 – 3.51 (m, 4H), 2.68 (t, $J = 5.4$ Hz, 2H), 2.46 (s, 4H); HRMS (ESI) m/z calcd for $C_{20}H_{24}N_7O_2S^+$ $[M+H]^+$: 426.17067; found: 426.17247.

5.2.1.4.

N-methyl-2-(4-((6-(1-methyl-1H-pyrazol-4-yl)-[1,2,4]triazolo[3,4-b][1,3,4]thiadiazol-3-yl)methyl)phenoxy)acetamide (4b)

White solid; Yield: 37%; m.p.: 243-245°C; 1H NMR (300 MHz, DMSO- d_6) δ 8.59 (s, 1H), 8.08 (d, $J = 0.8$ Hz, 1H), 7.99 (s, 1H), 7.33 – 7.23 (m, 2H), 6.97 – 6.87 (m, 2H), 4.42 (s, 2H), 4.33 (s, 2H), 3.93 (s, 3H), 2.63 (d, $J = 4.7$ Hz, 3H); ^{13}C NMR (75 MHz, DMSO- d_6) δ 168.42, 159.51, 157.13, 152.69, 146.99, 138.17, 132.25, 130.26(2C), 128.74, 115.30(2C), 112.41, 67.53, 39.51, 30.00, 25.80; HRMS (ESI) m/z calcd for $C_{17}H_{17}N_7O_2SNa^+$ $[M+Na]^+$: 406.10566; found: 406.10698.

5.2.1.5.

N,N-dimethyl-2-(4-((6-(1-methyl-1H-pyrazol-4-yl)-[1,2,4]triazolo[3,4-b][1,3,4]thiadiazol-3-yl)methyl)phenoxy)acetamide (4c)

White solid; Yield: 54%; m.p.: 170-172°C; 1H NMR (300 MHz, DMSO- d_6) δ : 8.59 (s, 1H), 8.08 (s, 1H), 7.25 (d, $J = 8.6$ Hz, 2H), 6.87 (d, $J = 8.6$ Hz, 2H), 4.76 (s, 2H), 4.33 (s, 2H), 3.32 (s, 3H), 2.98 (s, 3H), 2.83 (s, 3H); ^{13}C NMR (75 MHz, DMSO- d_6) δ 167.55, 159.51, 157.53, 152.68, 147.06, 138.18, 132.23, 130.08, 128.27, 115.15, 112.42, 66.19, 39.50, 36.03, 35.39, 30.00; HRMS (ESI) m/z calcd for $C_{18}H_{20}N_7O_2S^+$ $[M+H]^+$: 398.13937; found: 398.14084.

5.2.1.6.

3-(((7-methoxyquinolin-4-yl)oxy)methyl)-6-(1H-pyrrol-2-yl)-[1,2,4]triazolo[3,4-b][1,3,4]thiadiazole (**7a**)

Gray solid; Yield: 18%; m.p.: 205-206°C; ¹H NMR (300 MHz, DMSO-*d*₆) δ 12.38 (s, 1H), 8.73 (d, *J* = 5.3 Hz, 1H), 7.99 (d, *J* = 9.2 Hz, 1H), 7.35 (d, *J* = 2.6 Hz, 1H), 7.23 (d, *J* = 5.3 Hz, 1H), 7.16 (dt, *J* = 6.8, 2.5 Hz, 2H), 6.99 (s, 1H), 6.30 (dt, *J* = 4.4, 2.3 Hz, 1H), 5.77 (s, 2H), 3.90 (s, 3H); ¹³C NMR (75 MHz, DMSO-*d*₆) δ 160.97, 160.36, 159.86, 154.07, 152.35, 151.15, 143.30, 125.89, 123.33, 120.85, 118.72, 115.44, 111.25, 107.75, 101.21, 60.17, 55.89; HRMS (ESI) *m/z* calcd for C₁₈H₁₅N₆O₂S⁺ [M+H]⁺: 379.09717; found: 379.09795.

5.2.1.7.

3-(((7-methoxyquinolin-4-yl)oxy)methyl)-6-(1-methyl-1H-pyrrol-2-yl)-[1,2,4]triazolo[3,4-b][1,3,4]thiadiazole (**7b**)

White solid; Yield: 22%; m.p.: 214-215°C; ¹H NMR (300 MHz, DMSO-*d*₆) δ: 8.71 (d, *J* = 5.2 Hz, 1H), 8.04 (d, *J* = 9.2 Hz, 1H), 7.34 (d, *J* = 2.6 Hz, 1H), 7.29 – 7.12 (m, 3H), 6.95 (dd, *J* = 4.1, 1.7 Hz, 1H), 6.24 (dd, *J* = 4.0, 2.5 Hz, 1H), 5.85 (s, 2H), 3.90 (s, 3H), 3.81 (s, 3H); HRMS (ESI) *m/z* calcd for C₁₉H₁₇N₆O₂S⁺ [M+H]⁺: 393.11282; found: 393.11352.

5.2.1.8.

3-(((7-methoxyquinolin-4-yl)oxy)methyl)-6-(1H-pyrrol-3-yl)-[1,2,4]triazolo[3,4-b][1,3,4]thiadiazole (**7c**)

Brown solid; Yield: 14%; m.p.: 209-211°C; ¹H NMR (300 MHz, DMSO-*d*₆) δ: 11.76 (s, 1H), 8.73 (d, *J* = 5.3 Hz, 1H), 8.02 (d, *J* = 9.2 Hz, 1H), 7.71 (dt, *J* = 3.3, 1.8 Hz, 1H), 7.35 (d, *J* = 2.6 Hz, 1H), 7.27 – 7.11 (m, 2H), 6.99 (q, *J* = 2.4 Hz, 1H), 6.57 (q, *J* = 2.3 Hz, 1H), 5.81 (s, 2H), 3.90 (s, 3H); ¹³C NMR (75 MHz, DMSO-*d*₆) δ 163.77, 160.94, 160.37, 154.13, 152.30, 151.18, 143.26, 123.29, 122.17, 121.68, 118.68, 115.54, 113.70, 107.76, 107.11, 101.36, 60.39, 55.88; HRMS (ESI) *m/z* calcd for C₁₈H₁₅N₆O₂S⁺ [M+H]⁺: 379.09717; found: 379.09827.

5.2.1.9.

3-(((7-methoxyquinolin-4-yl)oxy)methyl)-6-(1-methyl-1H-pyrazol-4-yl)-[1,2,4]triazol

o[3,4-b][1,3,4]thiadiazole (**7d**)

Brown solid; Yield: 27%; m.p.: 203-205°C; ¹H NMR (300 MHz, DMSO-*d*₆) δ: 8.73 (d, *J* = 5.2 Hz, 1H), 8.62 (s, 1H), 8.09 (s, 1H), 8.01 (d, *J* = 9.2 Hz, 1H), 7.35 (d, *J* = 2.5 Hz, 1H), 7.23 (d, *J* = 5.3 Hz, 1H), 7.17 (dd, *J* = 9.2, 2.5 Hz, 1H), 5.81 (s, 2H), 3.92 (s, 3H), 3.90 (s, 3H); ¹³C NMR (75 MHz, DMSO-*d*₆) δ 170.09, 160.96, 160.38, 154.26, 152.23, 151.05, 143.39, 138.24, 132.43, 123.27, 118.72, 115.49, 112.25, 107.61, 101.30, 60.31, 55.89, 39.52; HRMS (ESI) *m/z* calcd for C₁₈H₁₆N₇O₂S⁺ [M+H]⁺: 394.10807; found: 394.11007.

5.2.1.10.

3-(((7-methoxyquinolin-4-yl)oxy)methyl)-6-(1-methyl-1H-indol-2-yl)-[1,2,4]triazolo[3,4-b][1,3,4]thiadiazole (**7e**)

Brown solid; Yield: 11%; m.p.: 232-234°C; ¹H NMR (300 MHz, DMSO-*d*₆) δ: 8.08 (d, *J* = 9.1 Hz, 1H), 7.70 (d, *J* = 8.1 Hz, 1H), 7.62 (d, *J* = 8.7 Hz, 1H), 7.49 – 7.33 (m, 3H), 7.25 (d, *J* = 5.4 Hz, 1H), 7.23 – 7.13 (m, 2H), 5.92 (s, 2H), 3.90 (s, 3H), 3.09 (s, 3H); HRMS (ESI) *m/z* calcd for C₂₃H₁₉N₆O₂S⁺ [M+H]⁺: 443.12847; found: 443.12930.

5.2.1.11.

6-(5-fluoro-1H-indol-2-yl)-3-(((7-methoxyquinolin-4-yl)oxy)methyl)-[1,2,4]triazolo[3,4-b][1,3,4]thiadiazole (**7f**)

White solid; Yield: 15%; m.p.: 236-238°C; ¹H NMR (300 MHz, DMSO-*d*₆) δ: 12.47 (s, 1H), 8.76 (dd, *J* = 5.3, 1.6 Hz, 1H), 8.07 – 7.97 (m, 1H), 7.52 – 7.31 (m, 4H), 7.31 – 7.23 (m, 1H), 7.17 (d, *J* = 9.1 Hz, 2H), 5.84 (s, 2H), 3.89 (d, *J* = 1.6 Hz, 3H); HRMS (ESI) *m/z* calcd for C₂₂H₁₆FN₆O₂S⁺ [M+H]⁺: 5447.10340; found: 447.10379.

5.2.1.12.

6-(5-methoxy-1H-indol-2-yl)-3-(((7-methoxyquinolin-4-yl)oxy)methyl)-[1,2,4]triazolo[3,4-b][1,3,4]thiadiazole (**7g**)

White solid; Yield: 11%; m.p.: 252-253°C; ¹H NMR (300 MHz, DMSO-*d*₆) δ: 12.22 (s, 1H), 8.75 (d, *J* = 5.2 Hz, 1H), 8.01 (d, *J* = 9.1 Hz, 1H), 7.40 – 7.31 (m, 2H), 7.31 – 7.22 (m, 2H), 7.20 – 7.13 (m, 1H), 7.11 (d, *J* = 2.6 Hz, 1H), 6.94 (dd, *J* = 8.7, 2.5 Hz, 1H), 5.82 (s, 2H), 3.89 (s, 3H), 3.77 (s, 3H); HRMS (ESI) *m/z* calcd for C₂₃H₁₉N₆O₃S⁺

[M+H]⁺: 459.12339; found: 459.12486.

5.2.1.13.

3-(((7-methoxyquinolin-4-yl)oxy)methyl)-6-(pyridin-4-yl)-[1,2,4]triazolo[3,4-b][1,3,4]thiadiazole (**7h**)

Light brown solid; Yield: 28%; m.p.: 228-229°C; ¹H NMR (300 MHz, DMSO-*d*₆) δ: 8.88 – 8.80 (m, 2H), 8.74 (d, *J* = 5.3 Hz, 1H), 8.05 (d, *J* = 9.1 Hz, 1H), 7.95 – 7.88 (m, 2H), 7.35 (d, *J* = 2.6 Hz, 1H), 7.25 (d, *J* = 5.3 Hz, 1H), 7.18 (dd, *J* = 9.2, 2.6 Hz, 1H), 5.91 (s, 2H), 3.90 (s, 3H); HRMS (ESI) *m/z* calcd for C₁₉H₁₅N₆O₂S⁺ [M+H]⁺: 391.09717; found: 391.09884.

5.2.1.14.

6-(4-methoxyphenyl)-3-(((7-methoxyquinolin-4-yl)oxy)methyl)-[1,2,4]triazolo[3,4-b][1,3,4]thiadiazole (**7i**)

White solid; Yield: 24%; m.p.: 184-186°C; ¹H NMR (300 MHz, Chloroform-*d*) δ: 8.66 (d, *J* = 5.5 Hz, 1H), 8.07 (d, *J* = 9.2 Hz, 1H), 7.73 (d, *J* = 8.9 Hz, 2H), 7.40 (d, *J* = 2.2 Hz, 1H), 7.08 (dd, *J* = 9.2, 2.5 Hz, 1H), 7.02 (d, *J* = 5.5 Hz, 1H), 6.94 (d, *J* = 8.9 Hz, 2H), 5.72 (s, 2H), 3.88 (s, 3H), 3.82 (s, 3H); ¹³C NMR (75 MHz, Chloroform-*d*) δ 167.42, 163.34, 161.14, 160.65, 154.75, 151.51, 151.09, 143.07, 128.97(2C), 123.16, 121.45, 118.67, 115.82, 114.88(2C), 106.96, 100.03, 59.77, 55.64, 55.48; HRMS (ESI) *m/z* calcd for C₂₁H₁₈N₅O₃S⁺ [M+H]⁺: 420.1125; found: 420.1143.

5.2.1.15.

6-(3-methoxyphenyl)-3-(((7-methoxyquinolin-4-yl)oxy)methyl)-[1,2,4]triazolo[3,4-b][1,3,4]thiadiazole (**7j**)

Yellow solid; Yield: 25%; m.p.: 201-203°C; ¹H NMR (300 MHz, DMSO-*d*₆) δ: 8.65 (d, *J* = 5.3 Hz, 1H), 8.05 (d, *J* = 9.2 Hz, 1H), 7.56-7.51 (m, 3H), 7.38-7.30 (m, 4H), 7.06-7.02 (m, 2H), 6.95 (d, *J* = 5.3 Hz, 1H), 5.70 (s, 2H), 3.85 (s, 3H), 3.78 (s, 3H); ¹³C NMR (75 MHz, Chloroform-*d*) δ 167.68, 161.12, 160.55, 160.22, 154.75, 151.60, 151.22, 143.24, 130.63, 130.20, 123.11, 119.77, 119.02, 118.68, 115.81, 112.02, 107.08, 100.01, 59.75, 55.62, 55.48; HRMS (ESI) *m/z* calcd for C₂₁H₁₈N₅O₃S⁺ [M+H]⁺: 420.11249; found: 420.11374.

5.2.1.16.

6-(4-fluorophenyl)-3-(((7-methoxyquinolin-4-yl)oxy)methyl)-[1,2,4]triazolo[3,4-b][1,3,4]thiadiazole (**7k**)

White solid; Yield: 24%; m.p.: 195-196°C; ¹H NMR (300 MHz, Chloroform-*d*) δ: 8.66 (d, *J* = 5.4 Hz, 1H), 8.06 (d, *J* = 9.2 Hz, 1H), 7.81 (dd, *J* = 8.5, 5.1 Hz, 2H), 7.36 (d, *J* = 2.4 Hz, 1H), 7.15 (d, *J* = 8.3 Hz, 2H), 7.10 – 7.03 (m, 1H), 6.98 (d, *J* = 5.4 Hz, 1H), 5.72 (s, 2H), 3.88 (s, 3H); ¹³C NMR (75 MHz, Chloroform-*d*) δ 167.13, 166.51, 163.74, 161.14, 161.14, 160.51, 154.73, 151.65, 151.28, 143.32, 129.59, 129.47, 125.38, 123.07, 118.69, 117.13, 116.83, 115.80, 107.12, 100.00, 59.74, 55.49; HRMS (ESI) *m/z* calcd for C₂₀H₁₅FN₅O₂S⁺ [M+H]⁺: 408.09250; found: 408.09302.

5.2.1.17.

6-(3-fluorophenyl)-3-(((7-methoxyquinolin-4-yl)oxy)methyl)-[1,2,4]triazolo[3,4-b][1,3,4]thiadiazole (**7l**)

Yellow solid; Yield: 17%; m.p.: 209-210°C; ¹H NMR (300 MHz, Chloroform-*d*) δ: 8.73 (d, *J* = 5.5 Hz, 1H), 8.14 (d, *J* = 9.2 Hz, 1H), 7.68 – 7.58 (m, 2H), 7.53 (td, *J* = 8.0, 5.3 Hz, 1H), 7.46 (d, *J* = 2.6 Hz, 1H), 7.37 – 7.30 (m, 1H), 7.16 (dd, *J* = 9.2, 2.5 Hz, 1H), 7.08 (d, *J* = 5.5 Hz, 1H), 5.82 (s, 2H), 3.95 (s, 3H); HRMS (ESI) *m/z* calcd for C₂₀H₁₅FN₅O₂S⁺ [M+H]⁺: 408.09250; found: 408.09461.

5.2.1.18.

3-(((7-methoxyquinolin-4-yl)oxy)methyl)-6-(3,4,5-trifluorophenyl)-[1,2,4]triazolo[3,4-b][1,3,4]thiadiazole (**7m**)

Yellow solid; Yield: 13%; m.p.: 233-235°C; ¹H NMR (300 MHz, DMSO-*d*₆) δ: 8.74 (d, *J* = 5.6 Hz, 1H), 8.13 (d, *J* = 9.2 Hz, 1H), 7.56-7.51 (m, 3H), 7.19 (dd, *J* = 9.2, 2.4 Hz, 1H), 7.12 (d, *J* = 5.6 Hz, 1H), 5.84 (s, 2H), 3.97 (s, 3H); HRMS (ESI) *m/z* calcd for C₂₀H₁₃F₃N₅O₂S⁺ [M+H]⁺: 444.07366; found: 444.07575.

5.2.2 General procedure for preparation of **8a-8c**

7c (200 mg, 0.53 mmol) and brominated alkane (1.06 mmol) were dissolved in 15 mL DMF, and then KOH (84 mg, 1.5 mmol) was added. The mixture was stirred at room temperature for 12 hours. 45 mL water was added to the reaction mixture and the mixture was extracted with EA (30mL×3). The organic layer was washed with brine (45mL×3), dried over Na₂SO₄ and concentrated. The residue was purified by silica gel

chromatography to afford **8a-8c**.

5.2.2.1.

6-(1-(2-methoxyethyl)-1H-pyrrol-3-yl)-3-(((7-methoxyquinolin-4-yl)oxy)methyl)-[1,2,4]triazolo[3,4-b][1,3,4]thiadiazole (**8a**)

White solid; Yield: 36%; m.p.: 141-142°C; ¹H NMR (300 MHz, DMSO-*d*₆) δ: 8.72 (d, *J* = 5.1 Hz, 1H), 8.02 (d, *J* = 9.2 Hz, 1H), 7.71 (t, *J* = 2.0 Hz, 1H), 7.35 (d, *J* = 2.6 Hz, 1H), 7.26 – 7.12 (m, 2H), 7.04 – 6.96 (m, 1H), 6.54 (dd, *J* = 3.0, 1.8 Hz, 1H), 5.80 (s, 1H), 4.12 (t, *J* = 5.2 Hz, 2H), 3.90 (s, 2H), 3.62 (t, *J* = 5.2 Hz, 2H), 3.24 (s, 2H); HRMS (ESI) *m/z* calcd for C₂₁H₂₁N₆O₃S⁺ [M+H]⁺: 437.13904; found: 437.13963.

5.2.2.2.

6-(1-(cyclopropylmethyl)-1H-pyrrol-3-yl)-3-(((7-methoxyquinolin-4-yl)oxy)methyl)-[1,2,4]triazolo[3,4-b][1,3,4]thiadiazole (**8b**)

White solid; Yield: 28%; m.p.: 131-133°C; ¹H NMR (300 MHz, DMSO-*d*₆) δ: 8.72 (d, *J* = 5.2 Hz, 1H), 8.02 (d, *J* = 9.2 Hz, 1H), 7.76 (s, 1H), 7.35 (d, *J* = 2.5 Hz, 1H), 7.26 – 7.11 (m, 2H), 7.06 (d, *J* = 2.6 Hz, 1H), 6.59 – 6.51 (m, 1H), 5.80 (s, 2H), 3.90 (s, 3H), 3.82 (d, *J* = 7.1 Hz, 2H), 1.25 – 1.16 (m, 1H), 0.57 – 0.48 (m, 2H), 0.37 (dd, *J* = 9.9, 4.8 Hz, 2H); HRMS (ESI) *m/z* calcd for C₂₂H₂₁N₆O₂S⁺ [M+H]⁺: 433.14412; found: 433.14559.

5.2.2.3.

6-(1-cyclopentyl-1H-pyrrol-3-yl)-3-(((7-methoxyquinolin-4-yl)oxy)methyl)-[1,2,4]triazolo[3,4-b][1,3,4]thiadiazole (**8c**)

White solid; Yield: 28%; m.p.: 81-82°C; ¹H NMR (300 MHz, DMSO-*d*₆) δ: 8.72 (d, *J* = 5.3 Hz, 1H), 8.02 (d, *J* = 9.2 Hz, 1H), 7.78 (t, *J* = 1.9 Hz, 1H), 7.35 (d, *J* = 2.6 Hz, 1H), 7.22 (d, *J* = 5.3 Hz, 1H), 7.17 (dd, *J* = 9.1, 2.5 Hz, 1H), 7.08 (t, *J* = 2.6 Hz, 1H), 6.55 (dd, *J* = 3.0, 1.8 Hz, 1H), 5.80 (s, 2H), 4.57 – 4.45 (m, 1H), 3.90 (s, 3H), 2.19 – 2.05 (m, 2H), 1.79 (s, 4H), 1.63 (s, 2H); HRMS (ESI) *m/z* calcd for C₂₃H₂₃N₆O₂S⁺ [M+H]⁺: 447.15977; found: 447.16079.

5.3 *In vitro* assays

5.3.1 Biochemical assay

Kinase inhibitory activities were determined using Hot-SpotSM kinase assay

performed by Reaction Biology Corp. (Malvern PA, USA). After the substrate was prepared in freshly prepared reaction buffer (20 mM Hepes pH 7.5, 10 mM MgCl₂, 1 mM EGTA, 0.02% Brij35, 0.02 mg/mL BSA, 0.1 mM Na₃VO₄, 2 mM DTT, 1% DMSO), 5 nM of human GST-tagged target kinase was delivered into the substrate solution and mixed gently. The testing compounds were dissolved in 100% DMSO to specific concentration and added into the kinase reaction mixture by Acoustic technology (Echo550; nanoliter range). The reaction mixture was incubated for 20 min at room temperature. ³³P-ATP (Specific activity 10 μCi/μL) was delivered into the reaction mixture to initiate the reaction and incubated at room temperature for 2 hours. The kinase activities were detected by filter-binding method. IC₅₀ values were obtained using Prism2 software (GraphPad).

5.3.2 In vitro cell activity assay

In vitro cell activity was determined using Cell Titer-Glo (CTG) assay [24-25]. SNU-5, EBC-1, MKN45 cells in exponential growth were plated onto each well of 96-well plate at a density of 4000 cells per well and maintained in RPMI-1640 media supplemented with 10% FPS. The cells were incubated in 5% CO₂ at 37 °C for 12 h. The tested compounds at the indicated final concentrations were added to the culture medium. The cells were then incubated at 37 °C under 5% CO₂ for 72 h. 50 μL CTG solution was added to each well and incubated at room temperature for 10 min. The fluorescence signal values were determined with Envision2104 plate reader. The % inhibitory was calculated as follows: cell inhibitory = $(1 - V_{\text{sample}} / V_{\text{vehicle control}}) \times 100\%$.

5.3.3 Western blot analysis

MKN45 cells in exponential growth were placed onto each well of 6-well plate at a density of 2x10⁴ cells per well and maintained in RPMI-1640 media supplemented with 10% FPS. Cells were then treated with ice-cold RIPA lysis buffer supplemented with a protease inhibitor cocktail to get whole-cell extracts. Protein concentration was determined by BCA assay. Cell lysate containing 30μg protein was separated by SDS-PAGE electrophoresis and transferred onto PVDF membranes. The membranes were blocked with 5% skim milk and incubated with primary antibodies

at 4 °C overnight. Membranes were then washed with TBST and incubated with horseradish peroxidase conjugated secondary antibody in 5% BSA in TBST for 1 h at room temperature. The membranes were visualized by ECL chemiluminescence system (Chemidoc XRS+, Bio-Rad, CA, USA).

5.4. Docking studies

Crystal structure of c-Met (PDB ID: 5YA5) was downloaded from the Protein Data Bank (www.rcsb.org). After the waters were deleted and the hydrogen atoms were added to the protein, the protein was prepared using Protein Preparation Wizard in the Schrodinger suite [26]. 3D structures of compounds **7d** was built and minimized by the Ligand Preparation module in Schrodinger. The Glide module with extra precision (XP) was selected for molecular docking. 10 best conformations were minimized by a post docking program. The image files were generated using pymol system.

Acknowledgments

This work was financially supported by the National Natural Science Foundation of China (Grant No. 81473078).

References

- [1] M. Dean, M. Park, M. M. Lebeau, T. S. Robins, M. O. Diaz, J. D. Rowley, D. G. Blair, G. F. Vandewoude, The human Met oncogene is related to the tyrosine kinase oncogenes. *Nature* 318 (1985) 385-388.
- [2] G. Manning, D. B. Whyte, R. Martinez, T. Hunter, S. Sudarsanam, The protein kinase complement of the human genome, *Science* 298 (2002) 1912-1934.
- [3] L. Trusolino, A. Bertotti, P. M. Comoglio, MET signaling: principles and functions in development, organ regeneration and cancer, *Nat. Rev. Mol. Cell Biol.* 11 (2010) 834–848.
- [4] F. Bladt, D. Riethmacher, S. Isenmann, A. Aguzzi, C. Birchmeier, Essential role for the c-met receptor in the migration of myogenic precursor cells into the limb bud, *Nature* 376 (1995) 768-771.
- [5] J. Chmielowiec, M. Borowiak, M. Morkel, T. Stradal, B. Munz, S. Werner, J.

- Wehland, C. Birchmeier, W. Birchmeier, c-Met is essential for wound healing in the skin, *J. Cell Biol.* 177 (2007) 151-162.
- [6] M. Kong-Beltran, S. Seshaqiri, J. Zha, W. Zhu, K. Bhawe, N. Mendoza, T. Holcomb, K. Pujara, J. Stinson, L. Fu, C. Severin, L. Rangell, R. Schwall, L. Amler, D. Wickramasinghe, R. Yauch, Somatic mutations lead to an oncogenic deletion of met in lung cancer, *Cancer Res.* 66 (2006) 283-289.
- [7] S. Corso, P. M. Comoglio, Cancer therapy: can the challenge be MET?, *Trends Mol. Med.* 11 (2005) 284-292.
- [8] L. Schmidt, F. M. Duh, F. Chen, T. Kishida, G. Glenn, P. Choyke, S. W. Scherer, Z. Zhuang, I. Lubensky, M. Dean, R. Allikmets, A. Chidambaram, U. R. Bergerheim, J. T. Feltis, C. Casadevall, A. Zamarron, M. Bernues, S. Richard, C. J. Lips, M. M. Walther, L. C. Tsui, L. Geil, M. L. Orcutt, T. Stackhouse, J. Lipan, L. Slife, H. Brauch, J. Decker, G. Niehans, M. D. Hughson, H. Moch, S. Storkel, M. I. Lerman, W. M. Linehan, B. Zbar, Germline and somatic mutations in the tyrosine kinase domain of the MET proto-oncogene in papillary renal carcinomas, *Nat. Genet.* 16 (1997) 68-73.
- [9] J. J. Cui, M. Trandubé, H. Shen, M. Nambu, P. P. Kung, M. Pairish, L. Jia, J. Meng, L. Funk, I. Botrous, M. Mctigue, N. Grodsky, K. Ryan, E. Padrique, G. Alton, S. Timofeevski, S. Yamazaki, Q. Li, H. Zou, J. Christensen, B. Mroczkowski, S. Bender, R. S. Kania, M. P. Edwards, Structure based drug design of crizotinib (PF-02341066), a potent and selective dual inhibitor of mesenchymal-epithelial transition factor (c-MET) kinase and anaplastic lymphoma kinase (ALK), *J. Med. Chem.* 54 (2011) 6342-6363.
- [10] S. Peters, A. A. Adjei, MET: a promising anticancer therapeutic target, *Nat. Rev. Clin. Oncol* 9 (2012) 314-326.
- [11] M. P. Lolkema, H. H. Bohets, H. T. Arkenau, A. Lampo, E. Barale, M. J. A. D. Jonge, L. V. Doorn, P. Hellemans, J. S. D. Bono, F. A. L. M. Eskens, The c-Met tyrosine kinase inhibitor JNJ-38877605 causes renal toxicity through species specific insoluble metabolite formation, *Clin. Cancer Res.* 21 (2015) 2297-2304.
- [12] A. A. Boezio, K. W. Copeland, K. Rex, B. K. Albrecht, D. Bauer, S. F. Bellon, C.

- Boezio, M. A. Broome, D. Choquette, A. Coxon, I. Dussault, S. Hirai, R. Lewis, M. J. Lin, J. Lohman, J. Liu, E. A. Peterson, M. Potashman, R. Shimanovich, Y. Teffera, D. A. Whittington, K. R. Vaida, J. C. Harmange, Discovery of (R)-6-(1-(8-Fluoro-6-(1-methyl-1H-pyrazol-4-yl)-[1,2,4]triazolo[4,3-a]pyridin-3-yl)ethyl)-3-(2-methoxyethoxy)-1,6-naphthyridin-5(6H)-one (AMG 337), a Potent and Selective Inhibitor of MET with High Unbound Target Coverage and Robust In Vivo Antitumor Activity, *J. Med. Chem.* 59 (2016) 2328-2342.
- [13] F. M. Yakes, J. Chen, J. Tan, K. Yamaguchi, Y. Shi, P. Yu, F. Qian, F. Chu, F. Bentzien, B. Cancilla, J. Orf, A. You, A. D. Laird, S. Engst, L. Lee, J. Lesch, Y. C. Chou, A. H. Joly, Cabozantinib (XL184), a novel MET and VEGFR2 inhibitor, simultaneously suppresses metastasis, angiogenesis, and tumor growth, *Mol. Cancer Ther.* 10 (2011) 2298-2308.
- [14] N. Munshi, S. Jeay, Y. Li, C. Chen, D. S. France, M. A. Ashwell, J. Hill, M. M. Moussa, D. S. Leggett, C. J. Li, ARQ 197, a Novel and Selective Inhibitor of the Human c-Met Receptor Tyrosine Kinase with Antitumor Activity, *Mol. Cancer Ther.* 9.6 (2010) 1544-1553.
- [15] J. J. Cui, Targeting receptor tyrosine kinase MET in cancer: small molecule inhibitors and clinical progress, *J. Med. Chem.* 57 (2013) 4427-4453.
- [16] X. Jiang, H. Liu, Z. Song, X. Peng, Y. Ji, Q. Yao, M. Geng, J. Ai, A. Zhang, Discovery and SAR study of c-Met kinase inhibitors bearing an 3-amino-benzo[d]isoxazole or 3-aminoindazole scaffold, *Bioorg. Med. Chem.* 23 (2015) 564-578.
- [17] W. Hu, B. Hiraikawa, B. Jessen, M. Lee, S. Aguirre, A tyrosine kinase inhibitor-induced myocardial degeneration in rats through off-target phosphodiesterase inhibition, *J. Appl. Toxicol.* 32 (2012) 1008-1020.
- [18] L. Zhang, B. Zhang, J. Zhao, Y. Zhi, L. Wang, T. Lu, Y. Chen, Structure-based design, synthesis, and evaluation of 4,5,6,7-tetrahydro-1H-pyrazolo[4,3-c]pyridine derivatives as novel c-Met inhibitors, *Eur. J. Med. Chem.* 138 (2017) 942-951.
- [19] H. Yuan, J. Zhuang, S. Hu, H. Li, J. Xu, Y. Hu, X. Xiong, Y. Chen, T. Lu,

- Molecular modeling of exquisitely selective c-Met inhibitors through 3D-QSAR and molecular dynamics simulations, *J. Chem. Inf. Model.* 54 (2014) 2544-2554.
- [20] H. Yuan, Q. Liu, L. Zhang, S. Hu, T. Chen, H. Li, Y. Chen, Y. Xu, T. Lu, Discovery, optimization and biological evaluation for novel c-Met kinase inhibitors, *Eur. J. Med. Chem.* 143 (2018) 491-502.
- [21] Y. Ma, G. Sun, D. Chen, X. Peng, Y. Chen, Y. Su, Y. Ji, J. Liang, X. Wang, L. Chen, J. Ding, B. Xiong, J. Ai, M. Geng, J. Shen, Design and optimization of a series of 1-sulfonylpyrazolo[4,3-b]pyridines as selective c-Met inhibitors, *J. Med. Chem.* 58 (2015) 2513-2529.
- [22] J. Liu, M. Nie, Y. Wang, J. Hu, F. Zhang, Y. Gao, Y. Liu, P. Gong, Design, synthesis and structure-activity relationships of novel 4-phenoxyquinoline derivatives containing 1,2,4-triazolone moiety as cMet kinase inhibitors, *Eur. J. Med. Chem.* 123 (2016) 431-446.
- [23] Y. Wang, J. Ai, Y. Wang, Y. Chen, L. Wang, G. Liu, M. Geng, A. Zhang, Synthesis and c-Met Kinase Inhibition of 3,5-Disubstituted and 3,5,7-Trisubstituted Quinolines: Identification of 3-(4-Acetylpiperazin-1-yl)-5-(3-nitrobenzylamino)-7-(trifluoromethyl)quinoline as a Novel Anticancer Agent, *J. Med. Chem.* 54 (2011) 2127-2142.
- [24] CellTiter-Glo® Luminescent Cell Viability Assay Technical Bulletin. <http://cn.promega.com> (accessed 16.5.10).
- [25] A. N. Hata, M. J. Niederst, H. L. Archibald, M. Gomez-Caraballo, F. M. Siddiqui, H. E. Mulvey, Y. E. Maruvka, F. Ji, H. C. Bhang, V. K. Radhakrishna, G. Siravegna, H. Hu, S. Raoof, E. Lockerman, A. Kalsy, D. Lee, C. L. Keating, D. A. Ruddy, L. J. Damon, A. S. Crystal, C. Costa, Z. Piotrowska, A. Bardelli, A. J. Iafrate, R. I. Sadreyev, F. Stegmeier, G. Getz, L. V. Sequist, A. C. Faber, J. A. Engelman, Tumor cells can follow distinct evolutionary paths to become resistant to epidermal growth factor receptor inhibition, *Nat. Med.* 22 (2016) 262-269.
- [26] L. Schrodinger, Schrodinger Software Suite, New York: Schrödinger, LLC, (2011).

Highlights:

1. A series of [1,2,4]triazolo[3,4-b][1,3,4]thiadiazole derivatives were designed and synthesized.
2. The target compounds showed potent antitumor activity.
3. Compound **7d** showed nanomolar c-Met kinase and subnanomolar cell growth inhibitory activity.
4. Compound **7d** inhibiting the phosphorylation of c-Met kinase in MKN45 cell line.
5. Compound **7d** was highly selective to c-Met with over 2500-fold selectivity.